

## Electronic Structures of Six-Coordinate Ferric Porphyrin Complexes with Weak Axial Ligands: Usefulness of $^{13}\text{C}$ NMR Chemical Shifts<sup>§</sup>

Akito Hoshino,<sup>‡</sup> Yoshiki Ohgo,<sup>†</sup> and Mikio Nakamura<sup>\*,†,‡</sup>

Department of Chemistry, School of Medicine, Toho University, Ota-ku, Tokyo 143-8540, Japan, and Division of Biomolecular Science, Graduate School of Science, Toho University, Funabashi 274-8510, Japan

Received August 11, 2004

$^1\text{H}$  NMR,  $^{13}\text{C}$  NMR, and EPR spectra of six-coordinate ferric porphyrin complexes  $[\text{Fe}(\text{Por})\text{L}_2]\text{ClO}_4$  with different porphyrin structures are presented, where porphyrins (Por) are planar 5,10,15,20-tetraphenylporphyrin (TPP), ruffled 5,10,15,20-tetraisopropylporphyrin (T<sup>r</sup>PrP), and saddled 2,3,7,8,12,13,17,18-octaethyl-5,10,15,20-tetraphenylporphyrin (OETPP), and axial ligands (L) are weak oxygen ligands such as pyridine-*N*-oxide, substituted pyridine-*N*-oxide, DMSO, DMF, MeOH, THF, 2-MeTHF, and dioxane. These complexes exhibit the spin states ranging from an essentially pure high-spin ( $S = 5/2$ ) to an essentially pure intermediate-spin ( $S = 3/2$ ) state depending on the field strength of the axial ligands and the structure of the porphyrin rings. Reed and Guiset reported that the pyrrole-H chemical shift is a good probe to determine the spin state in the spin admixed  $S = 5/2, 3/2$  complexes (Reed, C. A.; Guiset, F. *J. Am. Chem. Soc.* **1996**, *118*, 3281–3282). In this paper, we report that the chemical shifts of the  $\alpha$ - and  $\beta$ -pyrrole carbons can also be good probes to determine the spin state because they have shown good correlation with those of the pyrrole-H or pyrrole- $\text{C}_\alpha$ . By putting the observed or assumed pyrrole-H or pyrrole- $\text{C}_\alpha$  chemical shifts of the pure high-spin and pure intermediate-spin complexes into the correlation equations, we have estimated the carbon chemical shifts of the corresponding complexes. The orbital interactions between iron(III) and porphyrin have been examined on the basis of these chemical shifts, from which we have found that both the  $d_{xy}-a_{2u}$  interaction in the ruffled  $\text{Fe}(\text{T}^r\text{PrP})\text{L}_2^+$  and  $d_{xy}-a_{1u}$  interaction in the saddled  $\text{Fe}(\text{OETPP})\text{L}_2^+$  are quite weak in the high-spin and probably in the intermediate-spin complexes as well. Close inspection of the correlation lines has suggested that the electron configuration of an essentially pure intermediate-spin  $\text{Fe}(\text{T}^r\text{PrP})\text{L}_2^+$  changes from  $(d_{xy}, d_{yz})^3(d_{xz})^1(d_z)^1$  to  $(d_{xy})^2(d_{xz}, d_{yz})^2(d_z)^1$  as the axial ligand (L) changes from DMF to MeOH, THF, 2-MeTHF, and then to dioxane. Although the DFT calculation has indicated that the highly saddled intermediate-spin  $\text{Fe}(\text{OETPP})(\text{THF})_2^+$  should adopt  $(d_{xy}, d_{yz})^3(d_{xz})^1(d_z)^1$  rather than  $(d_{xy})^2(d_{xz}, d_{yz})^2(d_z)^1$  because of the strong  $d_{xy}-a_{1u}$  interaction (Cheng, R.-J.; Wang, Y.-K.; Chen, P.-Y.; Han, Y.-P.; Chang, C.-C. *Chem. Commun.* **2005**, 1312–1314), our  $^{13}\text{C}$  NMR study again suggests that  $\text{Fe}(\text{OETPP})(\text{THF})_2^+$  should be represented as  $(d_{xy})^2(d_{xz}, d_{yz})^2(d_z)^1$  because of the weak  $d_{xy}-a_{1u}$  interaction. The contribution of the  $S = 3/2$  state in all types of the spin admixed  $S = 5/2, 3/2$  six-coordinate complexes has been determined on the basis of the  $^{13}\text{C}$  NMR chemical shifts.

### Introduction

Elucidation of the electronic structures of iron porphyrin complexes is quite important to understand the function and

\* To whom correspondence should be addressed. E-mail: mnakamu@med.toho-u.ac.jp.

<sup>†</sup> Department of Chemistry, School of Medicine, Toho University.

<sup>‡</sup> Division of Biomolecular Science, Graduate School of Science, Toho University.

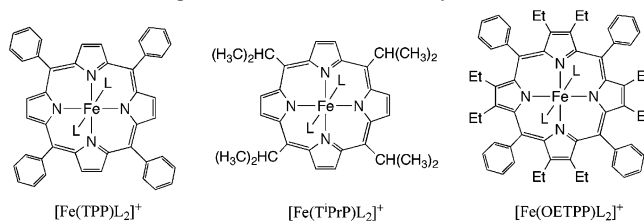
<sup>§</sup> Abbreviations. TPP, T<sup>r</sup>PrP, TETPrP, OEP, and OETPP: dianions of 5,10,15,20-tetraphenylporphyrin, 5,10,15,20-tetraisopropylporphyrin, 5,10,15,20-tetrakis(1-ethylpropyl)porphyrin, 2,3,7,8,12,13,17,18-octaethylporphyrin, and 2,3,7,8,12,13,17,18-octaethyl-5,10,15,20-tetraphenylporphyrin, respectively. 4-MePyNO, 3,5-Me<sub>2</sub>PyNO, PyNO, and 4-ClPyNO: 4-methylpyridine-*N*-oxide, 3,5-dimethylpyridine-*N*-oxide, pyridine-*N*-oxide, and 4-chloropyridine-*N*-oxide, respectively.

catalytic processes of naturally occurring heme proteins. A number of techniques have been used to solve this problem, which include UV–vis, NMR, EPR, resonance Raman, MCD, Mössbauer, EXAFS, SQUID, X-ray crystallography, etc.<sup>1</sup> Among these techniques,  $^1\text{H}$  NMR is particularly useful because it gives detailed information on the electronic structures of the complexes in solution at various temperatures. This is because the iron d orbital with an unpaired

- (1) (a) Que, L., Jr., Ed. *Physical Method in Bioinorganic Chemistry*, University Science Books, Sausalito, CA, 2000. (b) Solomon, E. I.; Lever, A. B. P., Eds. *Inorganic Electronic Structure and Spectroscopy*; John Wiley and Sons: New York, 1999; Vol 1.

electron interacts with the specific  $\pi$  molecular orbitals of porphyrin and increases the  $\pi$  spin density at the specific carbon and nitrogen atoms of the complex. Consequently, the NMR signals of the protons directly attached to or attached by two bonds to the carbon atoms exhibit an upfield or downfield shift. In addition, the unpaired electrons in the  $d_{x^2-y^2}$  and  $d_z^2$  orbitals can be delocalized through  $\sigma$  bonds to the protons and induce downfield shifts of the proton signals. Thus, we can determine which d orbital has unpaired electrons by the analysis of the observed  $^1\text{H}$  NMR chemical shifts. A number of good review articles have been published on the relationship between the electronic structures of iron porphyrins and the  $^1\text{H}$  NMR chemical shifts.<sup>2–7</sup> The  $^1\text{H}$  NMR spectroscopy has, however, an intrinsic deficit in a sense that the direct comparison of the chemical shifts in a wide variety of complexes is impossible. While the chemical shift of the proton directly bonded to the  $\beta$ -pyrrole carbon is a good probe to determine whether the complex has unpaired electron in the  $d_{x^2-y^2}$  orbital, the probe is not applicable to naturally occurring heme proteins because of the absence of such protons. In contrast, a direct comparison of the chemical shifts of three types of carbon atoms constituting the porphyrin ring, i.e., pyrrole- $\alpha$ , pyrrole- $\beta$ , and meso carbons, can be made by  $^{13}\text{C}$  NMR spectroscopy. Nevertheless, the systematic studies to reveal the relationship between the electronic structures and the chemical shifts of ferric porphyrin complexes has been hampered due to the low natural abundance and low sensitivity inherent to the  $^{13}\text{C}$  nucleus.<sup>6–17</sup> In the present work, we have determined both  $^1\text{H}$  and  $^{13}\text{C}$  NMR chemical shifts of a number of six-coordinate  $S = 5/2$ ,  $3/2$  complexes  $[\text{Fe}(\text{Por})\text{L}_2]^+$  ranging from a quite pure  $S = 5/2$  to a quite pure  $S = 3/2$ . The purpose of this study is to elucidate the contribution of the  $S = 3/2$  spin state at ambient temperature on the basis of the NMR chemicals

**Scheme 1.** Complexes Examined in This Study



shifts. We will especially emphasize the usefulness of the  $^{13}\text{C}$  NMR chemical shifts for the determination of the electronic structures of the complexes including the spin states and electron configurations. Scheme 1 shows the complexes examined in this study where the axial ligands (L's) are weak oxygen ligands such as 4-MePyNO, 3,5-Me<sub>2</sub>-PyNO, PyNO, 4-CIPyNO, DMSO, DMF, MeOH, THF, 2-MeTHF, and dioxane.

## Experimental Section

**General Procedure.** UV–vis spectra were measured on a SHIMADZU MultiSpec-1500 spectrophotometer at ambient temperature.  $^1\text{H}$  and  $^{13}\text{C}$  NMR spectra were recorded on a JEOL LA300 spectrometer operating at 300.4 MHz for  $^1\text{H}$ . Chemical shifts were referenced to the residual peak of dichloromethane (5.32 ppm for  $^1\text{H}$  and 53.8 ppm for  $^{13}\text{C}$ ). EPR spectra were measured at 4.2 K with a Bruker E500 spectrometer operating at X band and equipped with an Oxford helium cryostat. The concentrations of EPR samples were 5–8 mM. The  $g$  values were estimated by the simulation of the observed spectra.

**Synthesis.** Free base porphyrins such as H<sub>2</sub>(TPP), H<sub>2</sub>(TPrP), and H<sub>2</sub>(OETPP) were prepared by the literature methods.<sup>18,19</sup> Fe-(TPP)Cl, Fe(TPrP)Cl, and Fe(OETPP)Cl were prepared by the literature methods.<sup>20–22</sup> The perchlorate complexes Fe(Por)ClO<sub>4</sub> were prepared by the reaction between Fe(Por)Cl and AgClO<sub>4</sub> in THF solution. **Caution!** Perchlorate salts are potentially explosive when heated or shocked. Handle them in milligram quantities with care. The crude solid was purified by the recrystallization from dichloromethane and heptane. A series of six-coordinate complexes were obtained at ambient temperature by the addition of the CD<sub>2</sub>-Cl<sub>2</sub> solution of each ligand (L) into a CD<sub>2</sub>Cl<sub>2</sub> solution of Fe(Por)-ClO<sub>4</sub> or Fe(Por)(THF)<sub>2</sub>ClO<sub>4</sub> placed in an NMR sample tube. Addition of the ligand was continued until each signal showed no appreciable change in chemical shift.

## Results and Discussion

**Spectral Characteristics and Signal Assignments. i.  $^1\text{H}$  NMR Spectra.** Figure 1 shows the  $^1\text{H}$  NMR spectra of Fe-(TPrP)L<sub>2</sub><sup>+</sup> taken in CD<sub>2</sub>Cl<sub>2</sub> solution at 298 K where the axial ligands are (a) 3,5-Me<sub>2</sub>PyNO, (b) DMSO, (c) DMF, (d) MeOH, and (e) dioxane. The pyrrole signal moved upfield as the axial ligand was changed from 3,5-Me<sub>2</sub>PyNO (57.6

- (2) Walker, F. A. In *The Porphyrin Handbook*, Kadish, K. M., Smith, K. M., Guilard, R., Eds.; Academic Press: San Diego, CA, 2000; Vol. 5, Chapter 36, pp 81–183.
- (3) Walker, F. A. *Inorg. Chem.* **2003**, *42*, 4526–4544.
- (4) Walker, F. A. *Chem. Rev.* **2004**, *104*, 589–616.
- (5) Goff, H. M. Nuclear Magnetic Resonance of Iron Porphyrins. In *Iron Porphyrin*; Lever, A. B. P., Gray, H. B., Eds.; Physical Bioinorganic Chemistry Series 1; Addison-Wesley: Reading, MA, 1983; Vol. I, pp 237–281.
- (6) Bertini, I.; Luchinat, C. In *NMR of Paramagnetic Substances*. Lever, A. B. P., Ed.; Coordination Chemistry Reviews 150; Elsevier: Amsterdam, 1996; pp 29–75.
- (7) Bertini, I.; Luchinat, C. In *NMR of Paramagnetic Molecules in Biological Systems*; Lever, A. B. P., Gray, H. B., Eds.; Physical Bioinorganic Chemistry Series 3; Benjamin/Bumming: Menlo Park, CA, 1986; pp 165–229.
- (8) Wüthrich, K.; Baumann, R. *Helv. Chim. Acta* **1973**, *56*, 585–596.
- (9) Wüthrich, K.; Baumann, R. *Helv. Chim. Acta* **1974**, *57*, 336–350.
- (10) La Mar, G. N.; Viscio, D. B.; Smith, K. M.; Caughey, W. S.; Smith, M. L. *J. Am. Chem. Soc.* **1978**, *100*, 8085–8092.
- (11) Mispelter, J.; Momenteau, M.; Lhoste, J.-M. *J. Chem. Soc., Dalton Trans.* **1981**, 1729–1734.
- (12) Goff, H. M. *J. Am. Chem. Soc.* **1981**, *103*, 3714–3722.
- (13) Boersma, A. D.; Goff, H. *Inorg. Chem.* **1982**, *21*, 581–586.
- (14) Goff, H. M.; Shimomura, E. T.; Phillippi, M. A. *Inorg. Chem.* **1983**, *22*, 66–71.
- (15) Toney, G. E.; terHaar, L. W.; Savrin, J. E.; Gold, A.; Hatfield, W. E.; Sangaiah, R. *Inorg. Chem.* **1984**, *23*, 2561–2563.
- (16) Toney, G. E.; Gold, A.; Savrin, J. E.; terHaar, L. W.; Sangaiah, R. *Inorg. Chem.* **1984**, *23*, 4350–4352.
- (17) Mao, J.; Zhang, Y.; Oldfield, E. *J. Am. Chem. Soc.* **2002**, *124*, 13911–13920.

- (18) Wagner, R. W.; Lawrence, D. S.; Lindsey, J. S. *Tetrahedron Lett.* **1987**, *28*, 3069–3070.
- (19) Barkigia, K. M.; Berber, M. D.; Fajer, J.; Medforth, C. J.; Renner, M. W.; Smith, K. M. *J. Am. Chem. Soc.* **1990**, *112*, 8851–8857.
- (20) Cheng, R.-J.; Chen, P.-Y.; Gau, P.-R.; Chen, C.-C.; Peng, S.-M. *J. Am. Chem. Soc.* **1997**, *119*, 2563–2569.
- (21) Ikeue, T.; Ohgo, Y.; Saitoh, T.; Nakamura, M.; Fujii, H.; Yokoyama, M. *J. Am. Chem. Soc.* **2000**, *122*, 4068–4076.
- (22) Sparks, L. D.; Medforth, C. J.; Park, M.-S.; Chamberlain, J. R.; Ondrias, M. R.; Senge, M. O.; Smith, K. M.; Shelnutt, J. A. *J. Am. Chem. Soc.* **1993**, *115*, 581–592.

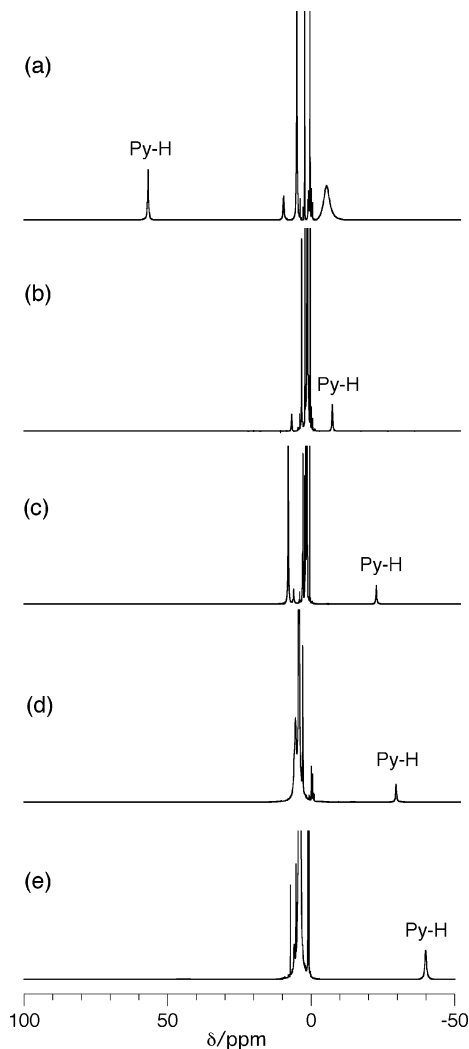


**Figure 1.**  $^1\text{H}$  NMR spectra of  $\text{Fe}(\text{TiPrP})\text{L}_2^+$  taken in  $\text{CD}_2\text{Cl}_2$  solution at 298 K where L's are (a) 3,5-Me<sub>2</sub>PyNO, (b) DMSO, (c) DMF, (d) MeOH, and (e) 1,4-dioxane. The broad signal at  $\delta$  -3.9 ppm in (a) is ascribed to the ligand protons.

ppm) to DMSO (-7.7 ppm), DMF (-21.5 ppm), MeOH (-28.3 ppm), and then to dioxane (-39.8 ppm). It is noteworthy that  $\text{Fe}(\text{TiPrP})(\text{dioxane})_2^+$  exhibits the pyrrole-H signal fairly upfield, -40 ppm, which should be compared with that of mono-aqua complex  $\text{Fe}(\text{TPP})(\text{H}_2\text{O})^+$ , -43 ppm in  $\text{C}_6\text{D}_6$  at 300 K, reported by Evans and Reed.<sup>23</sup> Signal assignment of  $\text{Fe}(\text{TPP})\text{L}_2^+$  and  $\text{Fe}(\text{TiPrP})\text{L}_2^+$  was carried out on the basis of the relative integral intensities and the signal widths. In the case of  $\text{Fe}(\text{OETPP})\text{L}_2^+$ , the ortho-H and one of the diastereotopic  $\text{CH}_2$  signals, both corresponding to 8H, appeared rather close to each other. Thus, the  $^1\text{H}$  NMR spectra of the corresponding phenyl deuterated complexes  $\text{Fe}(\text{OETPP})\text{L}_2^+-d_{20}$  were measured for the assignment. Figure 2 shows the  $^1\text{H}$  NMR spectra of  $\text{Fe}(\text{OETPP})(\text{THF})_2^+$  and  $\text{Fe}(\text{OETPP})(\text{THF})_2^+-d_{20}$  as a typical example, which enabled the assignment of all the signals. *Correction: The assignment of the ortho-H and one of the diastereotopic  $\text{CH}_2$  signals in  $\text{Fe}(\text{OETPP})(\text{THF})_2^+$  and analogous  $\text{Fe}(\text{OETPP})(4\text{-CNPy})_2^+$  in our previous papers should be reversed.*<sup>24–27</sup> Table 1 lists the chemical shifts of the complexes examined in this study. In Table 1, the axial ligands are arranged in descending order

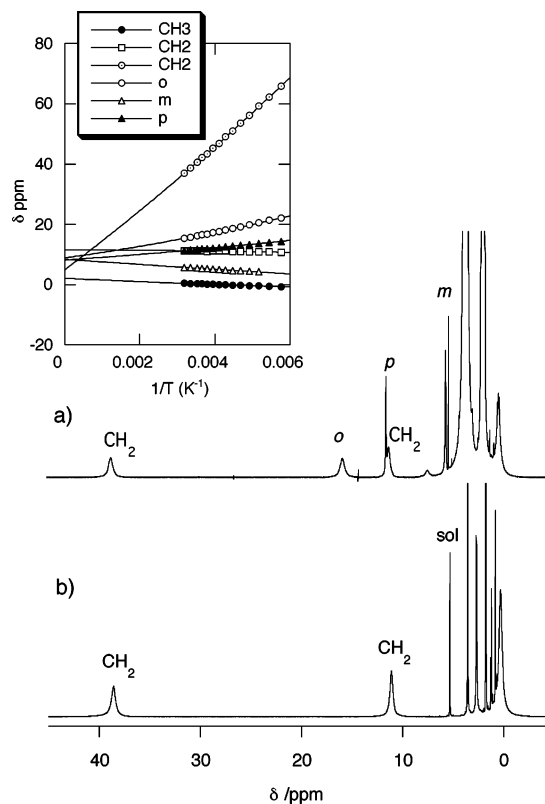


**Figure 2.**  $^1\text{H}$  NMR spectra of (a)  $\text{Fe}(\text{OETPP})(\text{THF})_2^+$  and (b)  $\text{Fe}(\text{OETPP})(\text{THF})_2^+-d_{20}$  taken in  $\text{CD}_2\text{Cl}_2$  solution at 298 K. Curie plots of each signal are given in the inset of (a).

of the pyrrole shifts, which indicates that the  $S = 3/2$  contribution increases on going from 4-MePyNO to THF.<sup>28</sup>

**ii.  $^{13}\text{C}$  NMR Spectra.** In the case of five-coordinate high-spin  $\text{Fe}(\text{TPP})\text{X}$ , the  $\alpha$  signal appears more upfield than the  $\beta$  signal; the chemical shifts of the  $\alpha$  and  $\beta$  signals in  $\text{Fe}(\text{TPP})\text{Cl}$  are 1205 and 1328 ppm, respectively.<sup>11,14</sup> The upfield shift of the  $\alpha$  relative to the  $\beta$  signal should be ascribed to the  $\pi$  spin densities at the neighboring meso carbon and nitrogen atoms caused by the  $d_z^2-a_{2u}$  interaction;<sup>29</sup> the  $a_{2u}$  orbital has large coefficients at the meso carbon and pyrrole nitrogen atoms, as shown in Scheme 2.<sup>2</sup> In the six-coordinate high-spin  $\text{Fe}(\text{TPP})\text{L}_2^+$ , however, the spin density at the meso carbon should decrease because of the less-favorable  $d_z^2-a_{2u}$  interaction. In fact, a fairly large upfield shift of the meso signal was observed in the high-spin six-coordinate complexes.<sup>14,30</sup> We can therefore expect a large downfield shift of the neighboring  $\alpha$  signals. Thus, the signals observed at the most downfield position in the

(23) Evans, D. R.; Reed, C. A. *J. Am. Chem. Soc.* **2000**, *122*, 4660–4667.

(24) As was pointed out,<sup>25</sup> the assignment of the ortho-H and one of the diastereotopic  $\text{CH}_2$  signals in analogous  $\text{Fe}(\text{OETPP})(4\text{-CNPy})_2^+$  in Table 2 of ref 26 and Table 1 of ref 27 has to be reversed.

(25) Yatsunyk, L. A.; Walker, F. A. *Inorg. Chem.* **2004**, *43*, 757–777.

(26) Ikeue, T.; Ohgo, Y.; Yamaguchi, T.; Takahashi, M.; Takeda, M.; Nakamura, M. *Angew. Chem., Int. Ed.* **2001**, *40*, 2617–2620.

(27) Ikeue, T.; Ohgo, Y.; Owendi, O.; Vicente, M. Graca. H.; Nakamura, M. *Inorg. Chem.* **2003**, *42*, 5560–5571.

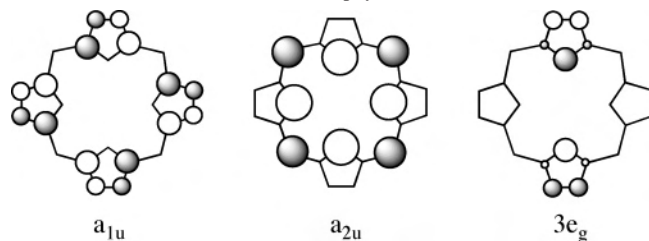
(28) Hoshino, A.; Nakamura, M. *Chem. Lett.* **2004**, *33*, 1234–1235.

(29) Cheng, R.-J.; Chen, P.-Y.; Lovell, T.; Liu, T.; Noodleman, L.; Case, D. A. *J. Am. Chem. Soc.* **2003**, *125*, 6774–6783.

(30) Nakamura, M.; Hoshino, A.; Ikezaki, A.; Ikeue, T. *Chem. Commun.* **2003**, 1862–1863.

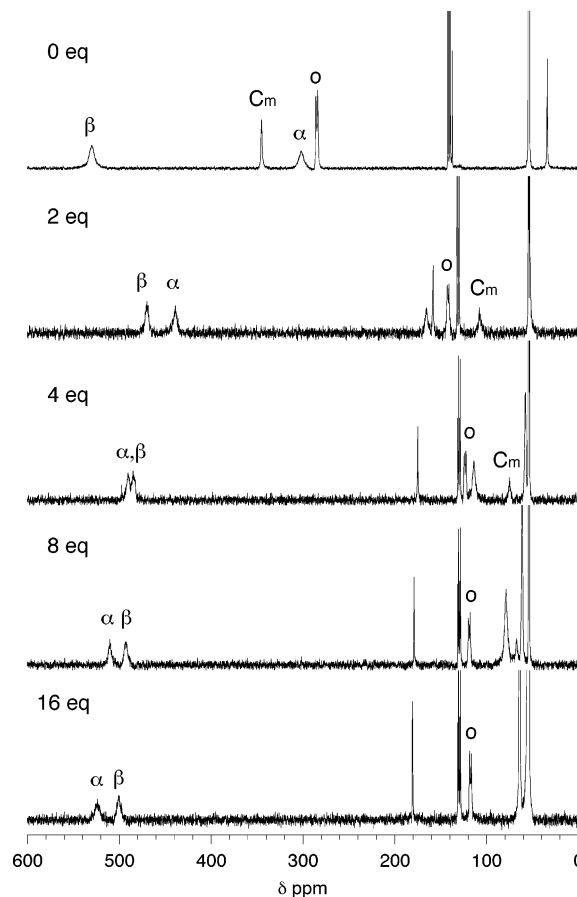
**Table 1.**  $^1\text{H}$  NMR Chemical Shifts ( $\text{CD}_2\text{Cl}_2$ , 298 K, ppm)

ligand	pyrrole			meso-Ar		
	H	$\text{CH}_\alpha$	$\text{CH}_\beta$	<i>o</i> ( $\text{H}_\alpha$ )	<i>m</i> ( $\text{H}_\beta$ )	<i>p</i>
	$\text{Fe}(\text{TPP})\text{L}_2^+$					
4-MePyNO	70.7	—	—	12.7	9.4	9.7
3,5-Me <sub>2</sub> PyNO	71.0	—	—	12.8	9.4	9.7
PyNO	68.9	—	—	13.3	9.5	9.8
4-ClPyNO	67.2	—	—	13.2	9.7	9.9
DMSO	67.2	—	—	13.0	9.6	9.7
DMF	60.2	—	—	13.5	9.9	9.9
MeOH	48.1	—	—	13.8	10.1	10.0
THF	3.1	—	—	14.1	10.1	10.3
	$\text{Fe}(\text{T}^i\text{PrP})\text{L}_2^+$					
4-MePyMO	58.5	—	—	(10.8)	(6.2)	—
3,5-Me <sub>2</sub> PyNO	57.6	—	—	(10.9)	(6.3)	—
PyNO	41.7	—	—	(9.9)	(6.1)	—
4-ClPyNO	35.2	—	—	(10.7)	(5.8)	—
DMSO	-7.7	—	—	(8.0)	(4.6)	—
DMF	-21.5	—	—	(7.3)	(4.2)	—
MeOH	-28.3	—	—	(7.3)	n.d.	—
THF	-35.5	—	—	(5.7)	(4.9)	—
2-MeTHF	-37.3	—	—	(6.4)	(5.7)	—
dioxane	-39.8	—	—	(5.9)	n.d.	—
	$\text{Fe}(\text{OETPP})\text{L}_2^+$					
4-MePyNO	—	21.0 44.2	2.4	14.7	8.7	10.3
3,5-Me <sub>2</sub> PyNO	—	18.6 43.8	2.4	14.7	8.7	10.4
PyNO	—	20.0 43.8	2.2	15.3	7.4	10.6
DMSO	—	15.4 39.2	0.9	17.2	7.4	10.6
DMF	—	11.6 37.7	-0.1	15.8	6.1	11.4
MeOH	—	11.7	0.3	15.8	5.9	11.5
THF	—	11.1	0.3	15.8	5.6	11.5
		38.7				

**Scheme 2.** Frontier Orbitals of Porphyrin

complexes with  $\text{L} = 4\text{-MePyNO}$ ,  $3,5\text{-Me}_2\text{PyNO}$ ,  $\text{PyNO}$ ,  $\text{DMSO}$ , and  $\text{DMF}$ , ranging from 1636 to 1474 ppm, were assigned to the  $\alpha$  carbons. Both the  $\alpha$  and  $\beta$  signal showed a large upfield shift in the THF complex due to the decrease in spin population in the  $d_{x^2-y^2}$  orbital. These signals were assigned by the titration method. Figure 3 shows the spectral change when THF was added to the  $\text{CD}_2\text{Cl}_2$  solution of  $\text{Fe}(\text{TPP})\text{ClO}_4$ . As THF was added, the signals at 302 and 530 ppm in  $\text{Fe}(\text{TPP})\text{ClO}_4$  shifted to the downfield and upfield positions and finally reached 547 and 518 ppm, respectively. Since the meso signal exhibited a large upfield shift from 345 to 60 ppm in the titration process, the signal that moved from 302 to 547 ppm was assigned to the neighboring  $\alpha$  carbons of  $\text{Fe}(\text{TPP})(\text{THF})_2^+$ .

Figure 4 shows the  $^{13}\text{C}$  NMR spectra of  $\text{Fe}(\text{T}^i\text{PrP})\text{L}_2^+$  taken in  $\text{CD}_2\text{Cl}_2$  solution at 298 K where the axial ligands are (a) 4-MePyNO, (b) DMSO, and (c) MeOH. The meso signals were assigned by the spectral comparison with the structurally analogous meso- $^{13}\text{C}$ -enriched  $\text{Fe}(\text{Te}^i\text{PrP})\text{L}_2^+$ .<sup>31</sup> In the  $\text{PyNO}$  and substituted  $\text{PyNO}$  complexes, the  $\alpha$  and  $\beta$

**Figure 3.** Spectral change when 2, 4, 8, and 16 equiv of THF was added to the  $\text{CD}_2\text{Cl}_2$  solution of  $\text{Fe}(\text{TPP})\text{ClO}_4$ . The  $\alpha$ ,  $\beta$ ,  $o$ , and  $\text{C}_m$  indicate the pyrrole- $\alpha$ , pyrrole- $\beta$ , ortho, and meso carbon signals, respectively.

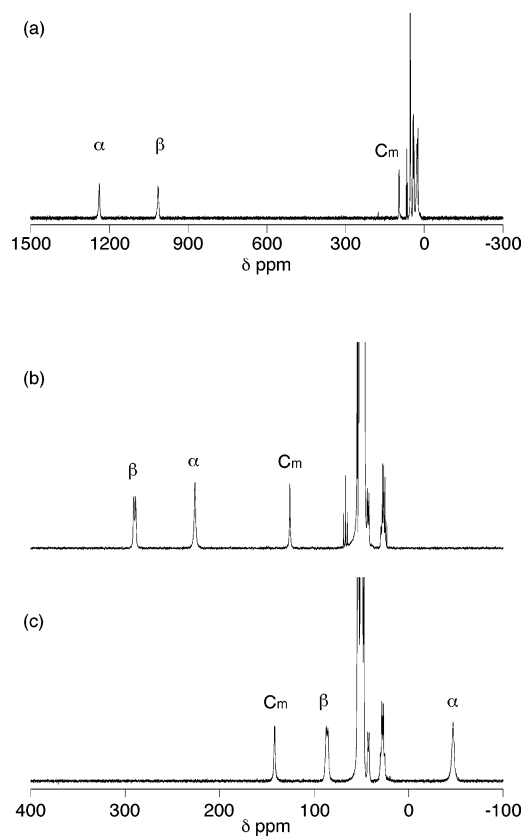
signals appeared rather downfield, as do those in  $\text{Fe}(\text{TPP})\text{L}_2^+$ . Thus, the most downfield-shifted signal was assigned to the  $\alpha$  signal. In the complexes with  $\text{L} = \text{DMSO}$ ,  $\text{DMF}$ ,  $\text{MeOH}$ ,  $\text{THF}$ , and  $\text{dioxane}$ , both the  $\alpha$  and  $\beta$  signals showed a large upfield shift. The signal assignment of these complexes was quite easy because the  $\beta$  signal exhibited clear doublet due to the  $\text{C-H}$  coupling as shown in Figure 4b and c.

Figure 5 shows the  $^{13}\text{C}$  NMR spectra of  $\text{Fe}(\text{OETPP})\text{L}_2^+$  taken under the same conditions where the axial ligands are (a) 4-MePyNO, (b) DMSO, and (c) THF. The meso signals were assigned unambiguously by the spectral comparison with the meso- $^{13}\text{C}$ -enriched  $\text{Fe}(\text{OETPP})\text{L}_2^+$ .<sup>31</sup> As shown in Figure 5, the line widths were quite different between the  $\alpha$  and  $\beta$  signals. Since the broad signal at 394 ppm in  $\text{Fe}(\text{OETPP})(\text{THF})_2^+$  was assigned to the  $\alpha$  signal on the basis of the titration method, the broad signals observed at the downfield position in other  $\text{Fe}(\text{OETPP})\text{L}_2^+$  were also assigned to the  $\alpha$  signals. Table 2 lists the chemical shifts of all the complexes examined in this study.<sup>32</sup>

**iii. EPR Spectra.** The EPR spectra were taken in frozen  $\text{CH}_2\text{Cl}_2$  solution at 4.2 K to obtain the additional information on the spin state. The  $g$  values were determined by the

(31) Sakai, T.; Ohgo, Y.; Ikeue, T.; Takahashi, M.; Takeda, M.; Nakamura, M. *J. Am. Chem. Soc.* **2003**, *125*, 13028–13029.

(32) Complete formation of  $\text{Fe}(\text{OETPP})(\text{THF})_2^+$  requires a large excess of THF. The meso carbon chemical shift reported previously, -244 ppm at 298 K, contains a small amount of  $\text{Fe}(\text{OETPP})\text{ClO}_4$ .<sup>31</sup>



**Figure 4.**  $^{13}\text{C}$  NMR spectra of  $\text{Fe}(\text{T}^i\text{PrP})\text{L}_2^+$  taken in  $\text{CD}_2\text{Cl}_2$  at 298 K where L's are (a) 4-MePyNO, (b) DMSO, and (c) MeOH.

computer simulation of the observed spectra. Figure 6 shows the EPR spectra of  $\text{Fe}(\text{T}^i\text{PrP})\text{L}_2^+$  where L's are 4-MePyNO, PyNO, DMF, and dioxane. The complexes with PyNO and substituted PyNO exhibited the  $g_{\perp}$  signal at 5.85–5.70. In contrast, the complexes with much weaker axial ligands such as DMSO, DMF, MeOH, THF, 2-MeTHF, and dioxane showed the broad  $g_{\perp}$  signals at 4.2–4.0 together with some much sharper peaks at 6.2–5.6 corresponding to the minor species. The populations of the minor species are less than 10%. Figure 7 also shows the EPR spectra of  $\text{Fe}(\text{OETPP})\text{L}_2^+$  where L's are 4-MePyNO, PyNO, DMF, and MeOH. The EPR spectrum of the 4-MePyNO complex exhibited three signals at  $g = 5.5$ , 4.5, and 2.0 as shown in Figure 7a. Computer simulation suggested the existence of two components. The major species have signals at 5.54 and 2.00, while the minor species have them at 4.50 and 2.00. The EPR spectrum of the PyNO complex also exhibited three signals at  $g = 5.73$ , 4.35, and 2.00. The computer simulation revealed that these signals are ascribed to the single species. In the case of the DMSO, DMF, MeOH, and THF complexes, they showed the broad  $g_{\perp}$  signals at 4.2–4.0. Table 3 lists the EPR  $g$  values of all the complexes examined in this study. All the EPR spectra of  $\text{Fe}(\text{T}^i\text{PrP})\text{L}_2^+$  and  $\text{Fe}(\text{OETPP})\text{L}_2^+$  are given in the Supporting Information together with some simulated spectra.

**Determination of the  $S = 3/2$  Character by  $^{13}\text{C}$  NMR Chemical Shifts.** We have then determined the contribution of the  $S = 3/2$  in the spin admixed ( $S = 5/2, 3/2$ ) complexes at 298 K on the basis of the  $^1\text{H}$  and  $^{13}\text{C}$  NMR chemical shifts.

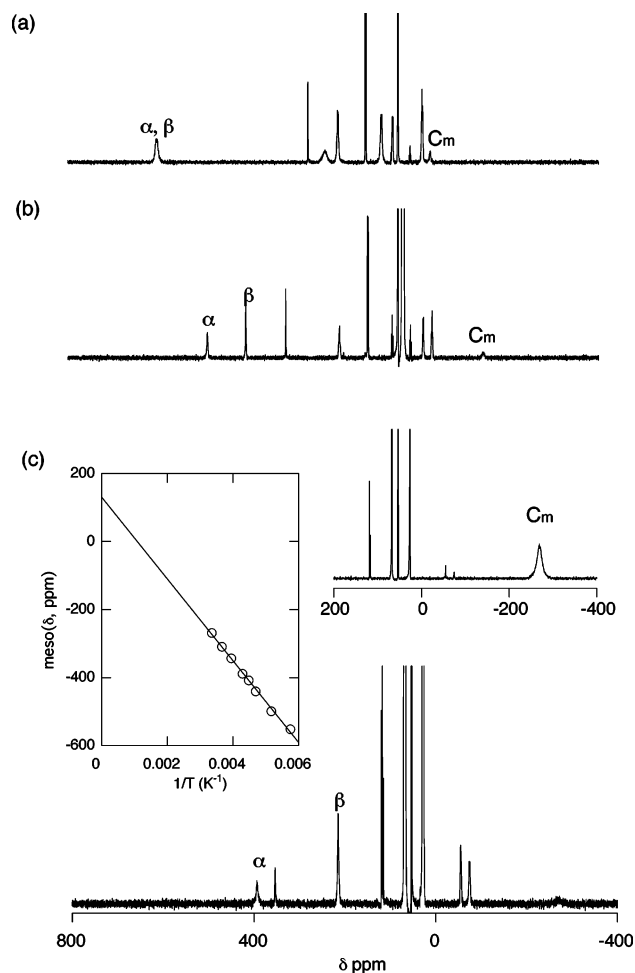


**Figure 5.**  $^{13}\text{C}$  NMR spectra of  $\text{Fe}(\text{OETPP})\text{L}_2^+$  taken in  $\text{CD}_2\text{Cl}_2$  solution at 298 K, where L's are (a) 4-MePyNO, (b) DMSO, and (c) THF.  $^{13}\text{C}$  NMR spectrum of meso- $^{13}\text{C}$  enriched  $\text{Fe}(\text{OETPP})(\text{THF})_2^+$  together with the Curie plots of the meso- $^{13}\text{C}$  signal is given in the inset of (c).

**i.  $[\text{Fe}(\text{TPP})\text{L}_2]\text{ClO}_4$ .** At first, we have examined the relationship of the chemical shifts between pyrrole-H and porphyrin carbons. The black lines in Figure 8a–c show the correlation of the chemical shifts of the pyrrole-H against those of the  $\alpha$  (○),  $\beta$  (□), and meso (△) carbons. The lines with the correlation coefficients 0.9989, 0.9982, and 0.8392 were obtained for these carbons, respectively. The results indicate that the chemical shifts of the  $\alpha$  and  $\beta$  carbons can be used as probes as well as those of the pyrrole-H to determine the spin state.<sup>3–7</sup> In contrast, the meso carbon shifts are less suitable to elucidate the  $S = 3/2$  contribution in the  $\text{Fe}(\text{TPP})\text{L}_2^+$  complexes.

We have then estimated the chemical shifts for the pure high-spin and intermediate-spin  $\text{Fe}(\text{TPP})\text{L}_2^+$  complexes. The six-coordinate complexes such as  $\text{Fe}(\text{TPP})(4\text{-MePyNO})_2^+$  and  $\text{Fe}(\text{TPP})(\text{PyNO})_2^+$  are considered to be in a quite pure high-spin state because the  $g_{\perp}$  values of these complexes are close to 6.0.<sup>33</sup> Thus, the chemical shift of the pyrrole-H in the pure high-spin  $\text{Fe}(\text{TPP})\text{L}_2^+$  was assumed to be 71 ppm. Although there is no example showing a pure intermediate-spin state in the six-coordinate  $\text{Fe}(\text{TPP})\text{L}_2^+$ , the five-

(33) Palmer, G. In *Iron Porphyrin, Part II*; Lever, A. B. P., Gray, H. B., Eds.; Addison-Wesley: Reading, MA, 1983; pp 43–88.

**Table 2.**  $^{13}\text{C}$  NMR Chemical Shifts of  $[\text{Fe}(\text{Por})\text{L}_2]\text{ClO}_4$  Taken in  $\text{CD}_2\text{Cl}_2$  at 298 K (ppm)

ligand	pyrrole				meso-Ar					Int(%)
	$\alpha$	$\beta$	$\text{C}_\alpha$	$\text{C}_\beta$	meso	<i>ip</i> ( $\text{C}_\alpha$ )	<i>o</i> ( $\text{C}_\beta$ )	<i>m</i>	<i>p</i>	
	$\text{Fe}(\text{TPP})\text{L}_2^+$									
4-MePyNO	1625	1248	—	—	26	171	122	129	129	~0
3,5-Me <sub>2</sub> PyNO	1636	1249	—	—	29	170	123	130	129	~0
PyNO	1617	1240	—	—	27	172	123	130	129	~0
4-ClPyNO	1594	1218	—	—	25	173	122	130	130	1.7
DMSO	1538	1226	—	—	10	168	127	130	129	4.8
DMF	1474	1179	—	—	13	170	(129–131)			8.3
MeOH	1261	1024	—	—	37	170	134	131	130	20
THF	547	518	—	—	60	181	117	129	130	59
	$\text{Fe}(\text{T}^i\text{PrP})\text{L}_2^+$									
4-MePyNO	1262	1038	—	—	97	(39)	(42)	—	—	22
3,5-Me <sub>2</sub> PyNO	1239	1015	—	—	97	(3)	(26)	—	—	23
PyNO	1031	865	—	—	110	(ca. 40)		—	—	36
4-ClPyNO	889	756	—	—	114	(42)	(30)	—	—	45
DMSO	226	290	—	—	126	(43)	(27)	—	—	87
DMF	24	138	—	—	145	(41)	(27)	—	—	100
MeOH	-47	86	—	—	142	(42)	(28)	—	—	100
THF	-122	22	—	—	115	(51)	(14)	—	—	100
2-MeTHF	-154	<sup>b</sup>	—	—	127	(46)	<sup>b</sup>	—	—	100
dioxane	-156	9	—	—	118	(49)	(18)	—	—	100
	$\text{Fe}(\text{OETPP})\text{L}_2^+$									
4-MePyNO <sup>a</sup>	598	601	-2	190	-19	257	66	126	127	42
3,5-Me <sub>2</sub> PyNO <sup>a</sup>	504	498	-14	191	-40	257	52	126	126	55
PyNO	555	512	-10	191	-63	278	38	125	125	51
DMSO	485	398	-24	186	-139	307	-4	122	122	66
DMF	419	250	-43	190	-221	338	-49	121	117	87
MeOH	409	239	-45	199	-211	343	-57	121	116	89
THF	394	215	-55	215	-269	354	-74	118	116	100

<sup>a</sup> The assignment of  $\alpha$  and  $\beta$  could be reversed. <sup>b</sup> Either  $\beta$  or  $\text{C}_\beta$  appears at 17 ppm.

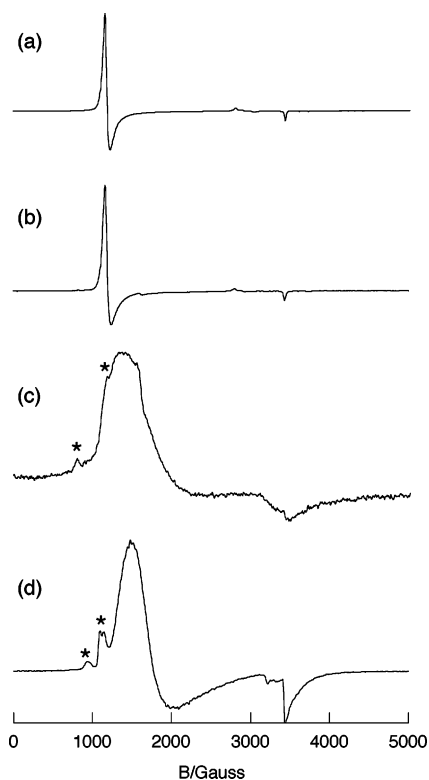


**Figure 6.** X-band EPR spectra of  $\text{Fe}(\text{T}^i\text{PrP})\text{L}_2^+$  taken in frozen  $\text{CH}_2\text{Cl}_2$  solution at 4.2 K where L's are (a) 4-MePyNO, (b) PyNO, (c) DMF, and (d) dioxane. Small signals signified by \* are ascribed to the minor components.

coordinate  $\text{Fe}(\text{TPP})(\text{OH}_2)^+$  reported by Evans and Reed is known to be the complex with high degree of the  $S = 3/2$  character on the basis of the Mössbauer parameters and effective magnetic moment.<sup>23</sup> Since the pyrrole-H chemical

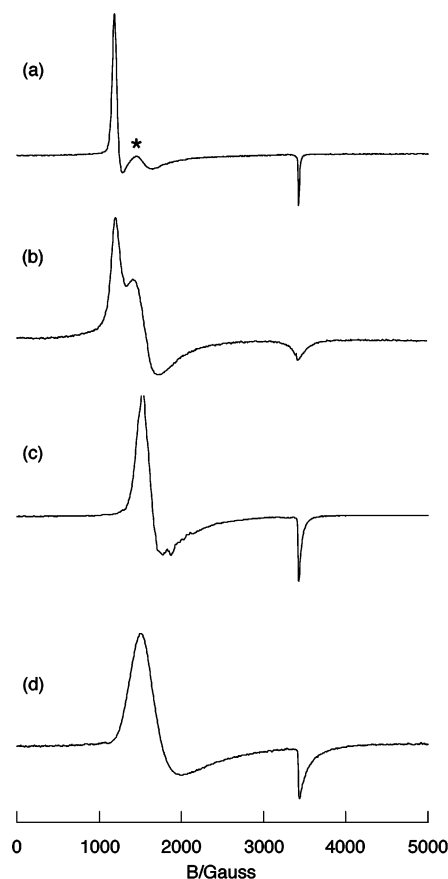


**Figure 7.** X-band EPR spectra of  $\text{Fe}(\text{OETPP})\text{L}_2^+$  taken in frozen  $\text{CH}_2\text{Cl}_2$  solution at 4.2 K, where L's are (a) 4-MePyNO, (b) PyNO, (c) DMF, and (d) MeOH. A small signal signified by \* is ascribed to the minor component.

shifts of five- and six-coordinate intermediate-spin complexes are supposed to be similar,<sup>34,35</sup> the pyrrole-H chemical shift

**Table 3.** EPR *g* Values (CH<sub>2</sub>Cl<sub>2</sub>, 4.2 K)

ligand	<i>g</i> values		ligand	<i>g</i> values	
	Fe(TPP)L <sub>2</sub> <sup>+</sup>				
4-MePyNO	6.11	5.81	DMF	5.85	2.00
3,5-Me <sub>2</sub> PyNO	5.85		MeOH	5.69	2.00
PyNO	6.00		THF <sup>a</sup>	4.59	2.00
4-ClPyNO	5.85			6.03	5.48
DMSO	5.85			2.01	
	Fe(T <sup>i</sup> PrP)L <sub>2</sub> <sup>+</sup>				
4-MePyNO	5.85		DMF <sup>c</sup>	4.2	2.00
3,5-Me <sub>2</sub> PyNO	5.70		MeOH <sup>c</sup>	4.1	2.00
PyNO	5.70		THF	4.0	1.97
4-ClPyNO	5.75		2-MeTHF <sup>c</sup>	4.1	2.00
DMSO <sup>b</sup>	4.2		dioxane <sup>d</sup>	4.1	2.00
	Fe(OETPP)L <sub>2</sub> <sup>+</sup>				
4-MePyNO <sup>e</sup>	5.54		DMSO <sup>b</sup>	4.2	2.01
3,5-Me <sub>2</sub> PyNO <sup>e</sup>	5.69		DMF	4.2	2.00
PyNO	5.73	4.35	MeOH	4.1	1.97
4-ClPyNO <sup>b</sup>	4.3		THF	4.0	2.00

<sup>a</sup> Two components are comparable in population. <sup>b</sup> A weak signal was observed at *g* = 5.6–5.8. The population of this species is less than 5%. <sup>c</sup> Some small signals were observed at 6.2–4.3. <sup>d</sup> Trace amount of high-spin species is contaminated. <sup>e</sup> A weak signal was observed at *g* = 4.5.

of Fe(TPP)(OH<sub>2</sub>)<sup>+</sup>, –43 ppm in C<sub>6</sub>D<sub>6</sub> at 300 K, was taken as the chemical shift for the intermediate-spin Fe(TPP)L<sub>2</sub><sup>+</sup> complex with axially coordinating oxygen ligand. By putting the assumed pyrrole-H shift (–43 ppm) of the pure intermediate-spin complex into the equations, we were able to estimate the chemical shifts of the α, β, and meso carbons to be –193, 24, and 84 ppm, respectively. The chemical shifts of the pure high-spin complex were taken from those of Fe(TPP)(4-MePyNO)<sub>2</sub><sup>+</sup> to be 1625 (α), 1248 (β), and 26 (meso) ppm. Thus, the contribution of the intermediate-spin state, Int(%), was determined on the basis of the pyrrole-α chemical shift by eq 1, where δ<sub>L</sub> is the observed α-carbon chemical shift of Fe(TPP)L<sub>2</sub><sup>+</sup>.

$$\text{Int}(\%) = [(1625 - \delta_L)/(1625 - (-193))] \times 100 \quad (1)$$

The Int(%) values for the DMSO, MeOH, and THF complexes were calculated to be 4.8, 20, and 59%, respectively, as listed in Table 2.

**[Fe(T<sup>i</sup>PrP)L<sub>2</sub>]ClO<sub>4</sub>.** We have examined the *S* = 3/2 contribution in the ruffled Fe(T<sup>i</sup>PrP)L<sub>2</sub><sup>+</sup> complexes. The chemical shifts of the Py-H in Table 1 indicate that the *S* = 3/2 character increases on going from the planar TPP to the ruffled T<sup>i</sup>PrP for all the axial ligands examined.<sup>28</sup> As in the case of Fe(TPP)L<sub>2</sub><sup>+</sup>, the chemical shifts of the α (○), β (□), and meso (Δ) carbon signals were plotted against those of the pyrrole-H signals as shown in panels a, b, and c of Figure 8, respectively; the red symbols are used for Fe(T<sup>i</sup>PrP)L<sub>2</sub><sup>+</sup>. Quite good linear fits were obtained for these carbons if the chemical shifts of the complexes with extremely weak axial ligands such as MeOH, THF, 2-MeTHF, and dioxane are omitted. They are shown in Figure 8 by the red lines. The

(34) The pyrrole-H chemical shifts of five-coordinate intermediate-spin complexes such as Fe(T<sup>i</sup>PrP)ClO<sub>4</sub> and Fe(TeTP)ClO<sub>4</sub> are –31.2 and –32.8 ppm, respectively, while those of the corresponding six-coordinate intermediate-spin complexes such as Fe(T<sup>i</sup>PrP)(THF)<sub>2</sub><sup>+</sup> and Fe(TeTP)(THF)<sub>2</sub><sup>+</sup> are –35.5 and –32.3 ppm, respectively.<sup>35</sup>

(35) Sakai, T.; Ohgo, Y.; Hoshino, A.; Ikeue, T.; Saitoh, T.; Takahashi, M.; Nakamura, M. *Inorg. Chem.* **2004**, *43*, 5034–5043.

correlation coefficients for the α, β, and meso carbons were 0.9996, 0.9993, and 0.9710, respectively. We noticed that the signals of the four complexes mentioned above showed a deviation from the correlation lines and that the deviation increased as the axial ligand changes from MeOH to THF, to 2-MeTHF, and then to dioxane as shown by the filled red marks.

We have then estimated the intrinsic chemical shifts for the high-spin Fe(T<sup>i</sup>PrP)L<sub>2</sub><sup>+</sup> complex. Although the 4-MePyNO complex showed the largest contribution of the *S* = 5/2 among the complexes examined in this study, it is still not in the pure high-spin state; the pyrrole-H shift at 298 K and EPR *g* at 4.2 K are 58.5 ppm and 5.85, respectively. We have assumed that the pyrrole-H signal of the pure high-spin Fe(T<sup>i</sup>PrP)L<sub>2</sub><sup>+</sup> should appear more downfield than that of the pure high-spin Fe(TPP)L<sub>2</sub><sup>+</sup>. This is because the unpaired electron in the d<sub>x<sup>2</sup>–y<sup>2</sup></sub> orbital can be delocalized to the pyrrole-H position more effectively in Fe(T<sup>i</sup>PrP)L<sub>2</sub><sup>+</sup> than in Fe(TPP)L<sub>2</sub><sup>+</sup> due to the shorter Fe–N<sub>p</sub> bond lengths in the former complexes; the average Fe–N<sub>p</sub> lengths in Fe(TPP)(THF)<sub>2</sub><sup>+</sup> and Fe(T<sup>i</sup>PrP)(THF)<sub>2</sub><sup>+</sup> are 2.016 and 1.967 Å, respectively.<sup>36,37</sup> In fact, the pyrrole-H signal in five-coordinate high-spin Fe(T<sup>i</sup>PrP)Cl appears at 90.4 ppm,<sup>38</sup> which is 10.0 ppm more downfield than that of high-spin Fe(TPP)Cl. Thus, we estimated the chemical shift of the pyrrole-H signal in high-spin Fe(T<sup>i</sup>PrP)L<sub>2</sub><sup>+</sup> to be 81 ppm, which is 10 ppm more downfield than that of high-spin Fe(TPP)(4-MePyNO)<sub>2</sub><sup>+</sup>. By putting the pyrrole-H shift (81 ppm) into the equations, we obtained the <sup>13</sup>C chemical shifts of the pure high-spin Fe(T<sup>i</sup>PrP)L<sub>2</sub><sup>+</sup>; they are 1610, 1290, and 87 ppm for the α, β, and meso carbons, respectively.

Determination of the intrinsic chemical shifts for the intermediate-spin complex was hampered because of the deviation of the chemical shifts from the correlation lines in the four complexes with L = MeOH, THF, 2-MeTHF, and dioxane. All of these complexes are supposed to be in an essentially pure intermediate-spin state at least at 4.2 K because the EPR *g*<sub>⊥</sub> values are in the range of 4.2–4.0.<sup>33</sup> In fact, one of these complexes, Fe(T<sup>i</sup>PrP)(THF)<sub>2</sub><sup>+</sup>, has been fully characterized as a quite pure intermediate-spin complex on the basis of the <sup>1</sup>H NMR, <sup>13</sup>C NMR, EPR, Mössbauer, and SQUID data.<sup>31,35,39</sup> Another fully characterized six-coordinate intermediate-spin complex is Fe(TMCP)(H<sub>2</sub>O)<sub>2</sub><sup>+</sup>, which shows the pyrrole signals at –33.7 and –36.3 ppm at 295 K in CDCl<sub>3</sub>–D<sub>2</sub>O solution.<sup>40</sup> Therefore, we were very much surprised when we found that the pyrrole-H signal of Fe(T<sup>i</sup>PrP)(dioxane)<sub>2</sub><sup>+</sup> appears at –39.8 ppm, which is 4.3 ppm more upfield than that of Fe(T<sup>i</sup>PrP)(THF)<sub>2</sub><sup>+</sup>. In the

(36) Chen, L.; Yi, G.-B.; Wang, L.-S.; Dharmawardana, U. R.; Dart, A. C.; Khan, M. A.; Richter-Addo, G. B. *Inorg. Chem.* **1998**, *37*, 4677–4688.

(37) Ohgo, Y.; Saitoh, T.; Nakamura, M. *Acta Crystallogr.* **2001**, *C57*, 233–234.

(38) Ikeue, T.; Ohgo, Y.; Uchida, A.; Nakamura, M.; Fujii, H.; Yokoyama, M.; *Inorg. Chem.* **1999**, *38*, 1276–1281.

(39) Ikeue, T.; Saitoh, T.; Yamaguchi, T.; Ohgo, Y.; Nakamura, M.; Takahashi, M.; Takeda, M. *Chem. Commun.* **2000**, 1989–1990.

(40) Simonato, J.-P.; Pecaut, J.; Le Pape, L.; Oddou, J.-L.; Jeandey, C.; Shang, M.; Scheidt, W. R.; Wojaczynski, J.; Wolowiec, S.; Latos-Grazynski, L.; Marchon, J.-C. *Inorg. Chem.* **2000**, *39*, 3978–3987.

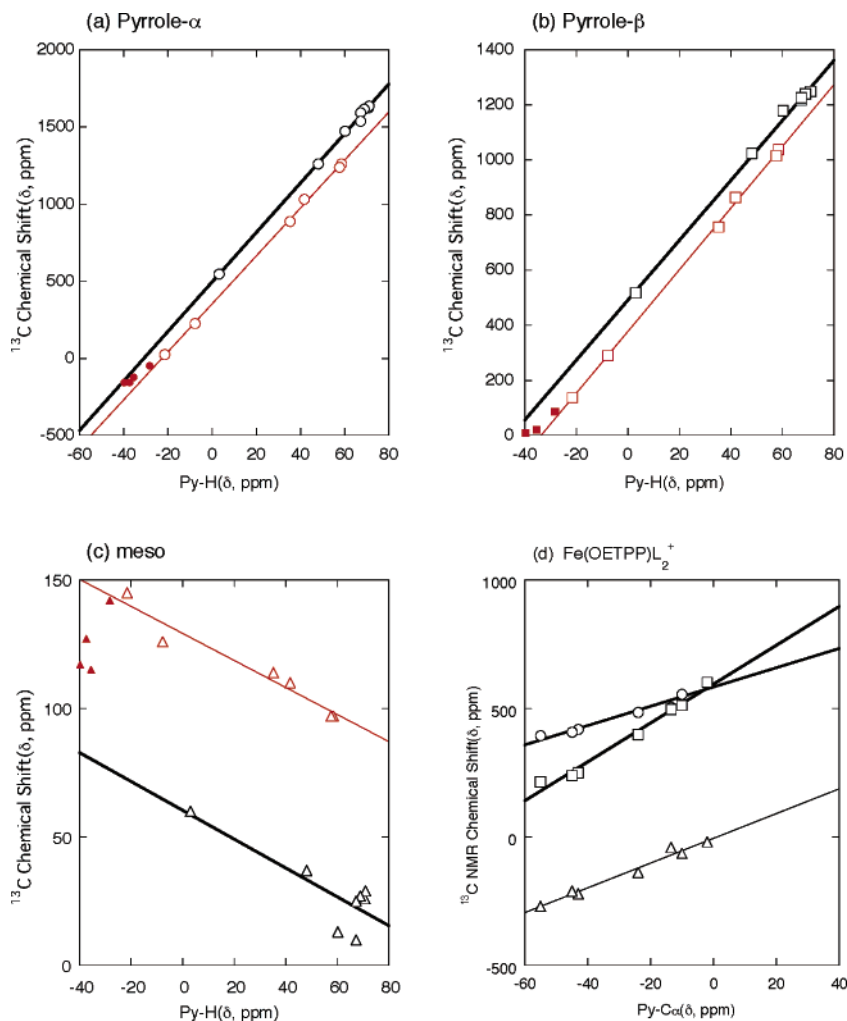


**Figure 8.** Chemical shift correlation. (a) Py-H vs Py- $\alpha$  in  $\text{Fe}(\text{TPP})\text{L}_2^+$  (black) and  $\text{Fe}(\text{T}'\text{PrP})\text{L}_2^+$  (red), (b) Py-H vs Py- $\beta$  in  $\text{Fe}(\text{TPP})\text{L}_2^+$  (black) and  $\text{Fe}(\text{T}'\text{PrP})\text{L}_2^+$  (red), (c) Py-H vs meso in  $\text{Fe}(\text{TPP})\text{L}_2^+$  (black) and  $\text{Fe}(\text{T}'\text{PrP})\text{L}_2^+$  (red), and (d) Py-C $\alpha$  vs Py- $\alpha$  (○), Py- $\beta$  (□), and meso (Δ) in  $\text{Fe}(\text{OETPP})\text{L}_2^+$ . The filled red marks in (a)–(c) correspond to the signals of  $\text{Fe}(\text{T}'\text{PrP})\text{L}_2^+$  where L's are MeOH, THF, 2-MeTHF, and dioxane.

previous paper, we reported that there are two types of intermediate-spin complexes with different electron configurations,  $S = 3/2(d_{xy})$  and  $S = 3/2(d_{\pi})$ , and that the highly ruffled  $\text{Fe}(\text{TEtPrP})(\text{THF})_2^+$  should adopt the  $S = 3/2(d_{xy})$  electron configuration;<sup>31</sup> the  $S = 3/2(d_{xy})$  and  $S = 3/2(d_{\pi})$  indicate the electron configurations of the intermediate-spin complexes represented as  $(d_{xz}, d_{yz})^3(d_{xy})^1(d_z)^1$  and  $(d_{xy})^2(d_{xz}, d_{yz})^2(d_z)^1$ , respectively. It is then expected that the difference in the pyrrole-H chemical shifts among the intermediate-spin complexes with ruffled porphyrin core should be ascribed to the difference in the  $S = 3/2(d_{xy})$  contribution. Thus, the upfield shift of the pyrrole-H shift observed when the axial ligand changes from DMF (−21.5 ppm), to MeOH (−28.3 ppm), to THF (−35.5 ppm), to 2-MeTHF (−37.3 ppm), and then to dioxane (−39.8 ppm) suggests that the contribution of the  $S = 3/2(d_{xy})$  decreases by this order. Close inspection of the data in Table 2 reveals that the meso signal continuously moves downfield from 97 to 145 ppm as the axial ligand changes from 4-MePyNO to DMF and reaches the maximum value in the DMF complex. When the axial ligand changes from DMF to dioxane, the meso signal shifts upfield from 145 to 117 ppm. The curious behavior of meso signal again supports for the change in electron configuration

from the  $S = 3/2(d_{xy})$  to the  $S = 3/2(d_{\pi})$ . Since the meso signal of  $\text{Fe}(\text{T}'\text{PrP})(\text{DMF})_2^+$  appears at the most downfield position, 145 ppm, we assumed that this complex adopts the purest  $S = 3/2(d_{xy})$  among the complexes examined in this study; a minor contribution from the  $S = 5/2$  and  $S = 3/2(d_{\pi})$  could not be neglected. Thus, we estimated the  $^{13}\text{C}$  chemical shifts of the  $\alpha$ ,  $\beta$ , and meso carbons of the pure  $S = 3/2(d_{xy})$  complex to be equal to those of the DMF complex; they are 24 ( $\alpha$ ), 138 ( $\beta$ ), and 145 (meso) ppm. The Int(%) is then expressed by eq 2 in the ruffled  $\text{Fe}(\text{T}'\text{PrP})\text{L}_2^+$  complexes with the  $S = 5/2$ ,  $3/2(d_{xy})$  spin system, on the basis of the pyrrole  $\alpha$  chemical shifts, where  $\delta_L$  is the observed  $\alpha$ -carbon chemical shift of  $\text{Fe}(\text{T}'\text{PrP})\text{L}_2^+$ .

$$\text{Int}(\%) = [(1610 - \delta_L)/(1610 - 24)] \times 100 \quad (2)$$

Thus, the Int(%) values for the 4-MePyNO, PyNO, DMSO, and DMF complexes were calculated to be 22, 37, 87, and 100%, respectively, as listed in Table 2. Similarly, if we assume that  $\text{Fe}(\text{T}'\text{PrP})(\text{dioxane})_2^+$  showing the pyrrole-H signal at the most upfield position (−39.8 ppm) is the pure  $S = 3/2(d_{\pi})$  complex, then the  $^{13}\text{C}$  chemical shifts of the  $\alpha$ ,  $\beta$ , and meso signals are −156, 9, and 117 ppm, respectively.



**Table 4.** Observed or Estimated  $^{13}\text{C}$  and  $^1\text{H}$  NMR Chemical Shifts of Pure High-Spin and Pure Intermediate-Spin  $\text{Fe}(\text{Por})\text{L}_2^+$  Complexes with three Different Porphyrin Structures<sup>a</sup>

spin state	porphyrin	$\alpha$ -C	$\beta$ -C	Py- $\text{C}_\alpha$	meso-C	pyrrole-H	examples
$S = 5/2$	TPP	<b>1625</b>	<b>1248</b>	—	<b>26</b>	<b>71</b>	$\text{Fe}(\text{TPP})(4\text{-MePyNO})_2^+$
	T <sup>i</sup> PrP	1610	1290	—	87	81	<sup>c</sup>
	OETPP	719	868	36	168	—	<sup>c</sup>
$S = 3/2$	TPP( $d_\pi$ ) <sup>b</sup>	-193	24	—	84	-43	<sup>c</sup>
	T <sup>i</sup> PrP( $d_\pi$ ) <sup>b</sup>	<b>-156</b>	<b>9</b>	—	<b>117</b>	<b>-40</b>	$\text{Fe}(\text{T}^i\text{PrP})(\text{Dioxane})_2^+$
	T <sup>i</sup> PrP( $d_{xy}$ ) <sup>b</sup>	<b>24</b>	<b>138</b>	—	<b>145</b>	<b>-22</b>	$\text{Fe}(\text{T}^i\text{PrP})(\text{DMF})_2^+$
	OETPP	<b>394</b>	<b>215</b>	<b>-55</b>	<b>-269</b>	—	$\text{Fe}(\text{OETPP})(\text{THF})_2^+$

<sup>a</sup> Bold entries are the observed chemical shifts. <sup>b</sup> The  $d_\pi$  and  $d_{xy}$  indicate the  $(d_{xy})^2(d_{xz}, d_{yz})^2(d_{z^2})^1$  and  $(d_{xy})^3(d_{yz})^1(d_{z^2})^1$  electron configurations, respectively. <sup>c</sup> The chemical shifts of the pyrrole-H and Py- $\text{C}_\alpha$  signals were estimated on the basis of the chemical shifts of the analogous complexes. Other chemical shifts were obtained from the correlation equations.

The contributions of the  $S = 3/2(d_{xy})$  in the intermediate-spin  $\text{Fe}(\text{T}^i\text{PrP})(\text{MeOH})_2^+$  and  $\text{Fe}(\text{T}^i\text{PrP})(\text{THF})_2^+$  are roughly estimated to be 60 and 20%, respectively.

iii. **[Fe(OETPP) $\text{L}_2$ ] $\text{ClO}_4$ .** Determination of the Int(%) value from the  $^1\text{H}$  NMR chemical shifts is much more difficult in  $\text{Fe}(\text{OETPP})\text{L}_2^+$  because the chemical shifts of the Py- $\text{CH}_2$  protons cannot be good probes to differentiate  $S = 3/2$  from  $S = 5/2$ . For example, the average Py- $\text{CH}_2$  shifts in  $\text{Fe}(\text{OETPP})\text{L}_2^+$  are not much different; they are 31.2, 31.9, 27.3, 24.4, and 24.9 ppm for  $\text{L} = 3,5\text{-Me}_2\text{PyNO}$ , PyNO, DMSO, MeOH, and THF, respectively; the axial ligands ( $\text{L}$ ) are arranged in descending order of the field-strength.<sup>28</sup> Similarly, the average  $\text{CH}_2$  shifts in  $\text{Fe}(\text{OETPP})\text{X}$  are 35.7, 34.0, 32.7, and 30.2 ppm for  $\text{X} = \text{F}^-$ ,  $\text{Cl}^-$ ,  $\text{Br}^-$ , and  $\text{I}^-$ , although the former two complexes are in the high-spin and the latter two are in the quite pure intermediate-spin state.<sup>41</sup> Relatively small ligand dependence of the  $\text{CH}_2$  shifts as compared with that of the pyrrole-H shifts in the spin admixed complexes can be explained in terms of the effect of spin delocalization through  $\sigma$  bonds. While the unpaired electron in the  $d_{x^2-y^2}$  orbital effectively delocalizes to the pyrrole-H positions through  $\sigma$  bonds, the delocalization to the Py- $\text{CH}_2$  positions must be greatly attenuated due to the presence of an additional  $\sigma$  bond. As a result, the upfield shift of the Py- $\text{CH}_2$  signals caused by the depopulation of the  $d_{x^2-y^2}$  orbital becomes much smaller than that of the pyrrole-H signals. In addition, the contact shift of the  $\text{CH}_2$  protons must be affected by the conformation of the ethyl group.<sup>6</sup> Since the conformation should change from complex to complex due to the steric interactions between ligand and the porphyrin core, the correlation between the  $\text{CH}_2$  chemical shifts and Fe(III) spin state is expected to be worse.

We have therefore examined the  $^{13}\text{C}$  NMR data to seek a better probe that can reflect the spin state of  $\text{Fe}(\text{OETPP})\text{L}_2^+$ . The Py- $\text{C}_\alpha$  seems to be the most plausible candidate because it is directly bonded to the  $\beta$  pyrrole carbon as in the case of the pyrrole-H. In addition, the conformational effect of the ethyl groups on the Py- $\text{C}_\alpha$  chemical shifts is supposed to be quite small as compared with that on the Py- $\text{CH}_2$ . Since  $\text{Fe}(\text{OETPP})(\text{THF})_2^+$  is known to be in an essentially pure intermediate-spin state, the chemical shift of the Py- $\text{C}_\alpha$  in  $\text{Fe}(\text{OETPP})(\text{THF})_2^+$ , -55.0 ppm, was taken as the chemical shift of the pure intermediate-spin complex.<sup>39</sup>

It is difficult, however, to determine the Py- $\text{C}_\alpha$  chemical shift of the pure high-spin complex because even  $\text{Fe}(\text{OETPP})(4\text{-MePyNO})_2^+$  exhibits the admixed intermediate-spin state; the  $g_\perp$  value of this complex was determined to be 5.54, as listed in Table 3. We tried to estimate the chemical shifts of the pure high-spin six-coordinate  $\text{Fe}(\text{OETPP})\text{L}_2^+$  on the basis of the reported chemical shifts of the analogous complexes. The chemical shifts of the Py- $\text{C}_\alpha$  in high-spin  $\text{Fe}(\text{OEP})\text{Cl}$  and  $\text{Fe}(\text{OEP})(\text{PyNO})_2^+$  are 79.2 and 57.5 ppm, respectively, indicating that the Py- $\text{C}_\alpha$  signal moves upfield by 21.7 ppm on going from high-spin five-coordinate to six-coordinate complex.<sup>42</sup> Since the average chemical shift of the Py- $\text{C}_\alpha$  signals in  $\text{Fe}(\text{OETPP})\text{Cl}$  is 57.8 ppm, the Py- $\text{C}_\alpha$  shift in hypothetical high-spin  $\text{Fe}(\text{OETPP})\text{L}_2^+$  is expected to be 36.1 ppm, which is 21.7 ppm more upfield than that of  $\text{Fe}(\text{OETPP})\text{Cl}$ . In the present discussion, we have approximated  $\text{Fe}(\text{OETPP})\text{Cl}$  as a high-spin complex at 298 K, though the EPR data at 4.2 K suggest ca. 5% contribution of the  $S = 3/2$  spin state.<sup>43</sup> The chemical shifts of the Py- $\text{C}_\alpha$  in  $\text{Fe}(\text{OETPP})\text{L}_2^+$  were then correlated with those of the  $\alpha$ ,  $\beta$ , and meso signals. The result is shown in Figure 8d. Quite good linearity was observed for the  $\alpha$ ,  $\beta$ , and meso carbon shifts; the correlation coefficients were 0.9755, 0.9906, and 0.9869, respectively. By putting the assumed Py- $\text{C}_\alpha$  shift (36 ppm) for the pure high-spin complex into the equations, we obtained the  $^{13}\text{C}$  chemical shifts of the  $\alpha$ ,  $\beta$ , and meso carbons to be 719 ( $\alpha$ ), 868 ( $\beta$ ), and 168 (meso) ppm. The chemical shifts of the pure intermediate-spin complex are taken from those of  $\text{Fe}(\text{OETPP})(\text{THF})_2^+$ . The Int(%) values can then be estimated on the basis of the  $\alpha$ ,  $\beta$ , meso, or Py- $\text{C}_\alpha$  chemical shifts. Equation 3 shows the Int(%) obtained on the basis of the Py- $\text{C}_\alpha$  chemical shifts:

$$\text{Int}(\%) = [(36 - \delta_L)/(36 - (-55))] \times 100 \quad (3)$$

Thus, the Int(%) values for the PyNO, DMSO, MeOH, and THF complexes were calculated to be 51, 66, 89, and 100%, respectively, as listed in Table 2.

**$^{13}\text{C}$  NMR Chemical Shifts of Pure High-Spin and Intermediate-Spin Complexes of Six-Coordinate  $\text{Fe}(\text{Por})\text{L}_2^+$ .** In Table 4, the chemical shifts of the pure high-spin and pure intermediate-spin six-coordinated  $\text{Fe}(\text{Por})\text{L}_2^+$  with

(42) Hoshino, A.; et al. unpublished results.

(43) Schünemann, V.; Gerdan, M.; Trautwein, A. X.; Haoudi, N.; Mandon, D.; Fischer, J.; Weiss, R.; Tabard, A.; Guillard, R. *Angew. Chem., Int. Ed.* **1999**, *38*, 3181.

(41) Nakamura, M.; Ikeue, T.; Ohgo, Y.; Takahashi, M.; Takeda, M. *Chem. Commun.* **2002**, 1198–1199.

three different porphyrin structures are listed. As mentioned in the previous section, the  $^{13}\text{C}$  and  $^1\text{H}$  chemical shifts in Table 4 were obtained either from the observed spectra or from the correlation lines shown in Figure 8. We will discuss the chemical shifts in Table 4 from the viewpoint of the iron–porphyrin orbital interactions.

In the high-spin TPP complex, the large downfield shifts of the  $\alpha$ -C,  $\beta$ -C, and Py-H signals can be explained in terms of the strong  $\sigma$ -donation of nitrogen atoms to the half filled  $d_{x^2-y^2}$  orbital.<sup>2–7</sup> If the planar TPP is replaced by the ruffled T'PrP, we can expect at least three factors that affect the  $^{13}\text{C}$  chemical shifts: (i) the contraction of the Fe–N bond,<sup>44,45</sup> (ii) the interaction between  $d_{xy}$  and  $a_{2u}$  orbitals,<sup>2,46</sup> and (iii) the interaction between  $d_{x^2-y^2}$  and  $a_{1u}$  orbitals.<sup>47,48</sup> Factor (i) induces further downfield shift to the  $\alpha$ ,  $\beta$ , and pyrrole-H signals, factor (ii) causes the downfield shift of the meso and upfield shift of the  $\alpha$  signal,<sup>21,49,50</sup> and factor (iii) would shift the  $\alpha$  and  $\beta$  signals to the downfield and the meso signal to the upfield positions; note that the  $a_{1u}$  orbital has large coefficients at the  $\alpha$  and  $\beta$  carbons and zero coefficient at the nitrogen and meso carbon atoms, as shown in Scheme 2. The data in Table 4 indicate the upfield shift of the  $\alpha$  and the downfield shift of the  $\beta$ , meso, and pyrrole-H signals, supporting the major contribution of factors (i) and (ii). It should be noted here that the downfield shift of the meso signal due to the  $d_{xy}$ – $a_{2u}$  interaction in the high-spin ruffled complexes is rather small, ca. 60 ppm, as compared with ca. 700 ppm in the corresponding low-spin complexes.<sup>49</sup>

If the planar TPP is replaced by the saddled OETPP, we can also expect at least three factors affecting the  $^{13}\text{C}$  NMR chemical shifts: (i) the less-effective nitrogen donation to the half filled  $d_{x^2-y^2}$  orbital, (ii) the interaction between the  $d_{x^2-y^2}$  and  $a_{2u}$  orbitals,<sup>51,52</sup> and (iii) the interaction between the  $d_{xy}$  and  $a_{1u}$  orbitals.<sup>47,48</sup> Factor (i) induces the upfield shift to the  $\alpha$  and  $\beta$  signals, factor (ii) causes the downfield shift of the meso and an upfield shift of the  $\alpha$  signal, and factor (iii) would shift the  $\alpha$  and  $\beta$  signals to the downfield and the meso signal to the upfield positions. The data in Table 2 suggest that factors (i) and (ii) mainly determine the  $^{13}\text{C}$  NMR chemical shifts; the  $\alpha$  and  $\beta$  signals shifted upfield

by 921 and 392 ppm, respectively, while the meso signal moved downfield by 147 ppm. In contrast, the  $d_{xy}$ – $a_{1u}$  interaction is supposed to be quite small in the high-spin saddled complexes.

We have then examined the orbital interactions in the intermediate-spin complexes. In the intermediate-spin TPP complex, the  $d_{\pi}$ – $3e_g$  interaction is considered to be the major interaction.<sup>2</sup> Since the  $3e_g$  orbital has relatively large coefficients at the pyrrole nitrogen and  $\beta$  carbon and zero coefficient at the meso carbon atoms, as shown in Scheme 2, we can expect the upfield shift of the  $\alpha$  signal. The expectation is confirmed by the data in Table 4; the chemical shift of the  $\alpha$  signal is estimated to be  $-193$  ppm. The large upfield shift of the pyrrole-H signal indicates that the complex adopts the  $S = 3/2(d_{\pi})$  electron configuration, which is further confirmed by the fact that the isotropic pyrrole-H shift of intermediate-spin  $\text{Fe}(\text{TPP})\text{L}_2^+$  ( $-52$  ppm) is twice as much as that of low-spin  $\text{Fe}(\text{TPP})(\text{HIm})_2^+$  ( $-26$  ppm); the latter complex is known to adopt the  $(d_{xy})^2(d_{xz}, d_{yz})^3$  electron configuration.

If the planar TPP is replaced by the ruffled T'PrP in the  $S = 3/2(d_{\pi})$  complexes, we can expect that the difference in the  $^{13}\text{C}$  NMR shifts should be rather small. In fact, the chemical shifts of these two complexes are quite similar, as shown in Table 4. If the electronic structure changes from the  $S = 3/2(d_{\pi})$  to the  $S = 3/2(d_{xy})$  in the ruffled complexes, one of the  $d_{\pi}$ – $3e_g$  interactions diminishes while the  $d_{xy}$ – $a_{2u}$  interaction occurs. It is expected that the loss of the  $d_{\pi}$ – $3e_g$  interaction should shift the  $\alpha$  signal downfield, while the occurrence of the  $d_{xy}$ – $a_{2u}$  interaction should shift the meso signal downfield. In fact, the data in Table 4 indicate that both the  $\alpha$  and meso signals showed downfield shifts by 173 and 28 ppm, respectively. Rather small downfield shift of the meso signal again suggests that the  $d_{xy}$ – $a_{2u}$  interaction is quite weak in the intermediate-spin complexes as in the case of the high-spin complexes. If the planar TPP is replaced by the saddled OETPP, the interaction between the filled  $a_{2u}$  and empty  $d_{x^2-y^2}$  orbital becomes possible in addition to the  $d_{\pi}$ – $3e_g$  interaction. As proposed by Cheng and co-workers, the former interaction could induce the negative spin to the  $a_{2u}$  orbital by the spin polarization mechanism.<sup>48</sup> As a result, the meso and  $\alpha$  signals move upfield and downfield, respectively.

**Electron Configurations of the Intermediate-Spin Complexes.** We have then examined the electron configuration of the intermediate-spin  $\text{Fe}(\text{OETPP})\text{L}_2^+$ . In the previous communication, we reported that the intermediate-spin  $\text{Fe}(\text{OETPP})(\text{THF})_2^+$  should adopt the  $S = 3/2(d_{\pi})$ .<sup>31</sup> We reached this conclusion on the basis of the unique  $^{13}\text{C}$  NMR chemical shifts of the low-spin  $\text{Fe}(\text{OETPP})\text{L}_2^+$ . An example is the chemical shifts of  $\text{Fe}(\text{OETPP})(\text{HIm})_2^+$  with the  $(d_{xy})^2(d_{xz}, d_{yz})^3$  electron configuration. This complex shows the  $\alpha$ ,  $\beta$ , and meso signals at 163, 167, and 7.0 ppm, respectively.<sup>49</sup> In contrast, the chemical shifts in  $\text{Fe}(\text{TPP})(\text{HIm})_2^+$  are very much different despite the same electron configuration; they are 39, 94, and 55 ppm for the  $\alpha$ ,  $\beta$ , and meso signals, respectively. Therefore, the large downfield shifts of the  $\alpha$  and  $\beta$  signals observed in  $\text{Fe}(\text{OETPP})(\text{THF})_2^+$  are consistent

- (44) Scheidt, W. R. In *The Porphyrin Handbook*, Kadish, K. M., Smith, K. M., Guillard, R., Eds.; Academic Press: San Diego, CA, 2000; Vol. 3, Chapter 16, pp 49–112.
- (45) Senge, M. O.; Bischoff, I.; Nelson, N. Y.; Smith, K. M. *J. Porphyrins Phthalocyanines* **1999**, *3*, 99–116.
- (46) Safo, M. K.; Walker F. A.; Raitsimring, A. M.; Walters, W. P.; Dolata, D. P.; Debrunner, P. G.; Scheidt, W. R. Safo, M. K.; Walker F. A.; Raitsimring, A. M.; Walters, W. P.; Dolata, D. P.; Debrunner, P. G.; Scheidt, W. R. *J. Am. Chem. Soc.* **1994**, *116*, 7760–7770.
- (47) Ghosh, A.; Vangberg, T.; Gonzalez, E.; Taylor, P. J. *J. Porphyrins Phthalocyanines* **2001**, *5*, 345–356.
- (48) Cheng, R.-J.; Wang, Y.-K.; Chen, P.-Y.; Han Y.-P.; Chang, C.-C. *Chem. Commun.* **2005**, 1312–1314.
- (49) Ikeue, T.; Ohgo, Y.; Saitoh, T.; Yamaguchi, T.; Nakamura, M. *Inorg. Chem.* **2001**, *40*, 3423–3434.
- (50) Ikeue, T.; Ohgo, Y.; Ongayi, O.; Vicente, G. H.; Nakamura, M. *Inorg. Chem.* **2003**, *42*, 5560–5571.
- (51) Renner, M. W.; Barkigia, K. M.; Zhang, Y.; Medforth, C. J.; Smith, K. M.; Fajer, J. *J. Am. Chem. Soc.* **1994**, *116*, 8582–8592.
- (52) Ghosh, A.; Harvorsen, I.; Nilsen, H. J.; Steene, E.; Wondimagegn, T.; Lie, R.; Caemelbecke, E. van; Guuo, N.; Ou, Z.; Kadish, K. M. *J. Phys. Chem. B* **2001**, *105*, 8120–8124.

with the existence of the two-half-filled  $d_{\pi}$  orbitals; the  $\alpha$ ,  $\beta$ , and meso signals appear at 394, 215, and  $-269$  ppm, respectively. Thus, we assigned the electron configuration of intermediate-spin  $\text{Fe}(\text{OETPP})(\text{THF})_2^+$  to be  $S = 3/2(d_{\pi})$  rather than  $S = 3/2(d_{xy})$ .

Recently, Cheng and co-workers proposed on the basis of the DFT calculation that the ground state of  $\text{Fe}(\text{OETPP})(\text{THF})_2^+$  should be represented as  $S = 3/2(d_{xy})$  rather than  $S = 3/2(d_{\pi})$ .<sup>48</sup> This is because the  $d_{xy}$  orbital is destabilized due to the interaction with the  $a_{1u}$  orbital which is possible in the saddled complexes. Since the  $a_{1u}$  orbital has relatively large coefficients at the  $\alpha$  and  $\beta$  carbons (especially on the  $\alpha$  carbon atoms) and zero coefficient at the meso carbon, the strong  $d_{xy}-a_{1u}$  interaction could induce the downfield shifts of the  $\alpha$  and  $\beta$  signals and the upfield shift of the meso signal. However, as we have already mentioned in this paper, the  $d_{xy}-a_{1u}$  interaction in the saddled complexes is quite weak in the high-spin, and probably in the intermediate-spin complexes as well because of the long  $\text{Fe}-\text{N}_p$  bond lengths. Furthermore, we noticed that the  $d_{xy}-a_{1u}$  interaction in the saddled complexes is rather weak even in the low-spin complexes with much shorter  $\text{Fe}-\text{N}_p$  bonds, which is exemplified in the chemical shifts of low-spin  $\text{Fe}(\text{OETPP})(\text{BuNC})_2^+$ . This complex is known to adopt the  $(d_{xz}, d_{yz})^4(d_{xy})^1$  electron configuration. Therefore, we can expect the downfield shifts of the  $\alpha$  and  $\beta$  signals and the upfield shift of the meso signal if the  $d_{xy}-a_{1u}$  interaction is fairly strong. Actually however, the  $\alpha$ ,  $\beta$ , and meso signals are observed at  $-5$ ,  $143$ , and  $417$  ppm, respectively, at  $298$  K.<sup>49</sup>

The electron configuration of the ruffled intermediate-spin  $\text{Fe}(\text{T}^i\text{PrP})(\text{THF})_2^+$  is also controversial. We reported in the previous paper that the complex adopts the  $S = 3/2(d_{xy})$  ground state.<sup>31</sup> Recent theoretical work suggested, however, that  $\text{Fe}(\text{T}^i\text{PrP})(\text{THF})_2$  should adopt the  $S = 3/2(d_{\pi})$  ground state.<sup>48</sup> The major reason is that the  $S = 3/2(d_{xy})$  complex should exhibit the meso signal fairly downfield due to the  $d_{xy}-a_{2u}$  interaction in the ruffled complex; the meso carbon chemical shift of  $\text{Fe}(\text{T}^i\text{PrP})(\text{THF})_2^+$  is  $115$  ppm at  $298$  K.<sup>31</sup> In the present study, we have found that the pyrrole-H signal in the essentially pure intermediate-spin  $\text{Fe}(\text{T}^i\text{PrP})\text{L}_2^+$  moved upfield from  $-22$  to  $-40$  ppm as the axial ligand changes from DMF to dioxane. Similarly, the meso-C signal moved upfield from  $145$  to  $117$  ppm for the same change in the axial ligand. We have ascribed the upfield shift of both the pyrrole-H and meso-C signals in a series of intermediate-spin  $\text{Fe}(\text{T}^i\text{PrP})\text{L}_2^+$  to the change in electronic state from  $S = 3/2(d_{xy})$  to  $S = 3/2(d_{\pi})$ . We have the impression that the two electronic states,  $S = 3/2(d_{xy})$  and  $S = 3/2(d_{\pi})$ , in ruffled  $\text{Fe}(\text{T}^i\text{PrP})\text{L}_2^+$  are quite close in energy and that they can easily be switched by the subtle change of axial ligand. Obviously, further experimental and theoretical studies are necessary to fully understand the electron configurations of the intermediate-spin complexes with nonplanar porphyrin cores.

**Factors Affecting the  $S = 3/2$  Character in the Six-Coordinate Spin Admixed Intermediate-Spin Complexes.** As mentioned, we have estimated the population of the  $S = 3/2$  in the  $S = 5/2, 3/2$  complexes  $\text{Fe}(\text{Por})\text{L}_2^+$  with various

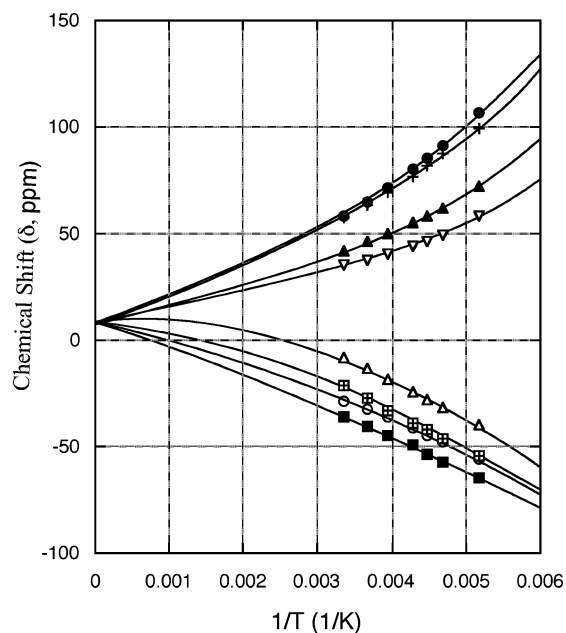


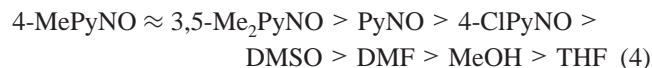
**Figure 9.** Curie plots of the pyrrole-H signals of  $\text{Fe}(\text{T}^i\text{PrP})\text{L}_2^+$ : ●, 4-MePyNO; +, 3,5-Me<sub>2</sub>PyNO; ▲, PyNO; ▽, 4-CIPyNO; △, DMSO; ■, DMF; ○, MeOH; ■, THF.

weak oxygen ligands and three different porphyrin structures. We have then considered to extract the factors affecting the population of the  $S = 3/2$  in these six-coordinate ferric porphyrin complexes.

**i. Axial Ligands.** In the five-coordinate ferric porphyrin complexes with anionic axial ligands, it is well established that the population of the  $S = 3/2$  in the admixed intermediate-spin complexes increases as the field strength of the anionic ligand is weakened. Thus, Reed and Guiset ranked the relative field strengths of weak anionic ligands on the basis of the pyrrole-H chemical shifts and called the hierarchy as magnetochemical series.<sup>53</sup> Similar to the five-coordinate complexes, the determination of the  $S = 3/2$  character in the six-coordinate complexes could be a good method to evaluate the weakness of the axial ligands. In the previous communication, we ranked the weakness of neutral ligands with oxygen as a coordinating atom on the basis of the pyrrole-H chemical shifts; part of the data is included in Table 1.<sup>28</sup> Although the field strengths of PyNO and alkyl-substituted PyNO's were difficult to determine in the planar TPP complexes because of the similarity of the chemical shifts, they were clearly discriminated in highly ruffled  $\text{T}^i\text{PrP}$  complexes. Figure 9 shows the Curie plots of the pyrrole-H of a series of  $\text{Fe}(\text{T}^i\text{PrP})\text{L}_2^+$ . The Curie lines were drawn so that they intercept the ordinate at the diamagnetic position of the pyrrole-H. The complexes with mainly  $S = 5/2$  showed the positive slope while those with mainly  $S = 3/2$  exhibited the negative slope. Thus, we were able to rank the field strength of a number of oxygen-containing ligands by using both planar TPP and ruffled  $\text{T}^i\text{PrP}$  complexes. It should be noted that the order of the shifts is maintained in a wide range of temperatures, as shown in Figure 9. The curvature of the Curie lines suggests that the population of

(53) Reed, C. A.; Guiset, F. *J. Am. Chem. Soc.* **1996**, *118*, 3281–3282.

the  $S = 3/2$  (or  $S = 5/2$ ) changes depending upon the temperature.<sup>54</sup> The field strength of these ligands is arranged in descending order, as shown in eq 4, and they are listed in Tables 1–3 by the same order.



It is clear that the ligands with formally charged oxygen atom such as PyNO are stronger than those with uncharged oxygen such as MeOH and THF. A substituent effect is also clearly seen since 4-MePyNO is stronger than and 4-ClPyNO is weaker than unsubstituted PyNO. Among eight ligands examined, THF is the weakest ligands. Thus, bis(THF) complex always shows the largest population of the  $S = 3/2$  state in a series of  $\text{Fe}(\text{Por})\text{L}_2^+$ .

**ii. Deformation of the Porphyrin Ring.** As mentioned in our previous papers, the  $S = 3/2$  spin state is stabilized in highly deformed porphyrin complexes, which is ascribed to the destabilization of the  $d_{x^2-y^2}$  orbital.<sup>39,40,53,55</sup> In fact, while all the bis(THF) complexes with deformed porphyrin ring such as OETPP and T'PrP exhibited a quite pure intermedi-

ate-spin state,  $\text{Fe}(\text{TPP})(\text{THF})_2^+$  showed an admixed intermediate-spin state with 68%  $S = 3/2$  contribution at 298 K. In the case of the ruffled porphyrin complexes, the paired electrons of four nitrogen atoms can effectively interact with the iron  $d_{x^2-y^2}$  orbital to destabilize this orbital. In the case of the saddled porphyrin complexes, the overlap between the nitrogen lone pair and the iron  $d_{x^2-y^2}$  orbital could be less effective due to the saddled core. However, the interaction between the iron  $d_{x^2-y^2}$  and porphyrin  $a_{2u}$  orbital becomes symmetry allowed.<sup>52</sup> As a result, the  $d_{x^2-y^2}$  orbital is also destabilized in the saddled complexes. The data in Tables 1–3 indicate that the Int(%) values actually increased on going from the planar TPP to the deformed T'PrP and OETPP cores.<sup>20,39–41,55</sup>

**Acknowledgment.** This work was supported by the Grant in Aid (No 14540521, 16550061) for Scientific Research from Ministry of Education, Culture, Sports, Science and Technology, Japan. Thanks are due to the Research Center for Molecular-Scale Nanoscience, the Institute for Molecular Science (IMS).

**Supporting Information Available:** EPR spectra of  $\text{Fe}(\text{T'PrP})\text{L}_2^+$  and  $\text{Fe}(\text{OETPP})\text{L}_2^+$  and simulation of some EPR spectra. This material is available free of charge via the Internet at <http://pubs.acs.org>.

IC0488942

(54) Nasset, M. J. M.; Cai, S.; Shokhireva, T. K.; Shokhirev, N. V.; Jacobson, S. E.; Jayaraj, K.; Gold, A.; Walker, F. A. *Inorg. Chem.* **2000**, *39*, 532–540.

(55) Barkigia, K. M.; Renner, M. W.; Fajer, J. J. *J. Porphyrins Phthalocyanins* **2001**, *5*, 415–418.